

Proportional Counter

- Secondary ionization occurs due to higher electric fields.

charge collected \propto primary ionization

- In a cylindrical electric field, kinetic energy gained by an electron between collisions at r_1 and r_2 is:

$$\Delta T_{\text{kin}} = e \int_{r_1}^{r_2} E(r) dr = e V_0 \frac{\ln \left(\frac{r_2}{r_1} \right)}{\ln \left(\frac{r_c}{r_w} \right)}$$

$(r_c = \text{radius of cathode}; r_w = \text{radius of wire})$

If $\Delta T_{\text{kin}} > W$ for the gas, secondary ionization takes place.

- But, high field strengths are present only very close to the anode wire.

So, in most of the region, the electric field just makes the e^- and ions to simply drift towards the electrodes.

And, multiplication and avalanche formation occurs very close to the anode (within a few wire radii)

- The primary ionization N_e is amplified by a "gas amplification factor" A

The voltage pulse at the electrode:

$$\Delta V = -A \cdot \frac{N_e}{C} \quad (C = \text{Capacitance})$$

- # of electron-ion pairs/cm³ produced by an electron is called First "Townsend Coefficient" α .

$$\alpha = \sigma_i \cdot N_A / V \quad \left(\begin{array}{l} \sigma_i = \text{Collision cross section} \\ \text{producing ionization} \\ N_A = \text{Avogadro No.} \\ V = \text{Molar volume} \end{array} \right)$$

and $dN(x) = \alpha \cdot N(x) dx$

$$\therefore N(x) = N_0 e^{\alpha x} \quad (N_0 = \text{Number of primary electrons})$$

More generally, since α depends on \vec{E} and hence x ,

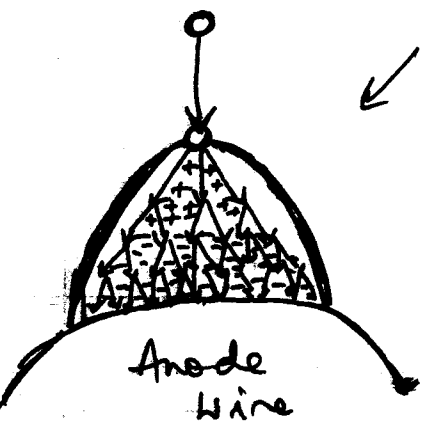
$$N(x) = N_0 e^{\int \alpha(x) dx}$$

Gas amplification,

$$A = \exp\left(\int_{r_L}^{r_i} \alpha(x) dx\right) \quad \left| \begin{array}{l} \text{Typically,} \\ A \approx 10^4 - 10^5 \end{array} \right.$$

r_L = radius where \vec{E} is above critical value for charge multiplication

Avalanche formation near the Anode wire



Lateral diffusion of electrons & ions cause a drop-shaped avalanche.
The electron & ion clouds drift apart.

Pulses/signals generated by e^- at the anode

$$\begin{aligned}\Delta U^- &= - \frac{Nq}{C} \int_{r_0}^{r_w} E(r) dr = - \frac{Nq}{C} \cdot \frac{U_0}{\ln(r_c/r_w)} \cdot \int_{r_0}^{r_w} \frac{dr}{r} \\ &= - \frac{Nq}{C} \cdot U_0 \cdot \frac{\ln(r_w/r_0)}{\ln(r_c/r_w)}\end{aligned}$$

||| by for ions;

$$\Delta U^+ = - \frac{Nq}{C} \cdot U_0 \cdot \frac{\ln(r_c/r_0)}{\ln(r_c/r_w)}$$

$$\begin{aligned}\therefore R \doteq \frac{\Delta U^+}{\Delta U^-} &= \frac{\ln(r_c/r_w)}{\ln(r_w/r_0)} = \frac{\ln(r_c/r_w)}{\ln(\frac{r_w + k\lambda}{r_w})} \\ &= \frac{\ln(r_c/r_w)}{k\lambda/r_w}\end{aligned}$$

$$\text{For } r_c = 20\text{mm}; r_w = 0.1\text{mm}, k\lambda = 0.02\text{ mm}; R = 25$$

Photon production due to de-excitation of atoms

can add to further ionization or amplification of the signal

$$N_0 A_Y = N_0 A + N_0 A^2 Y + N_0 A^3 Y^2 + \dots$$

$$= N_0 A \sum_{k=0}^{\infty} (AY)^k = \frac{N_0 A}{1 - YA}; \boxed{A_Y = \frac{A}{1 - YA}}$$

A_Y = Second Townsend coefficient

(γ = probability to produce one photoelectron/electron)

Photon feedback: Photons reaching cathode can release electrons, which in turn can get accelerated and generate avalanches.

So, "quenching" gases which have large photo absorption cross-sections (in the visible and UV) are added. Examples: CO_2 and CH_4 .

Ion feedback:

Ions reaching cathode can produce similar effect by releasing photons and electrons.

Quenchers help here as well.

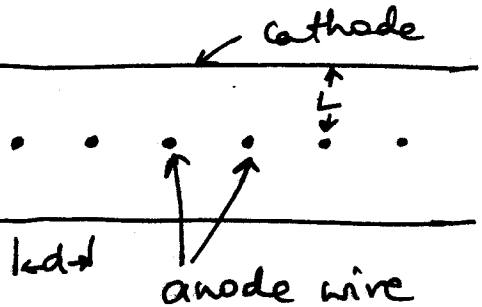


\therefore Ions of the quencher gas reach the cathode.

They have lower ionization and excitation potential. So, they do not stimulate a secondary emission.

Multi-Wire Proportional Chambers: (MWPC)

- A planar layer of proportional counters without separating walls



Used mostly to determine spatial coordinates of particles passing through.

Typically,

anodes: $10 - 30 \mu\text{m}$ gold-plated tungsten wire

d = distance between wires \sim a few mm

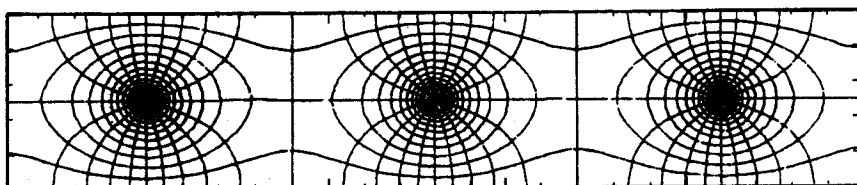
L = distance between anode & cathode $\sim 1 \text{ cm}$

Cathodes: metal foils or stretched wires

Gas mixtures: Noble gas + quencher

Gas amplification $\sim 10^5$

Electric fields are modified as below:

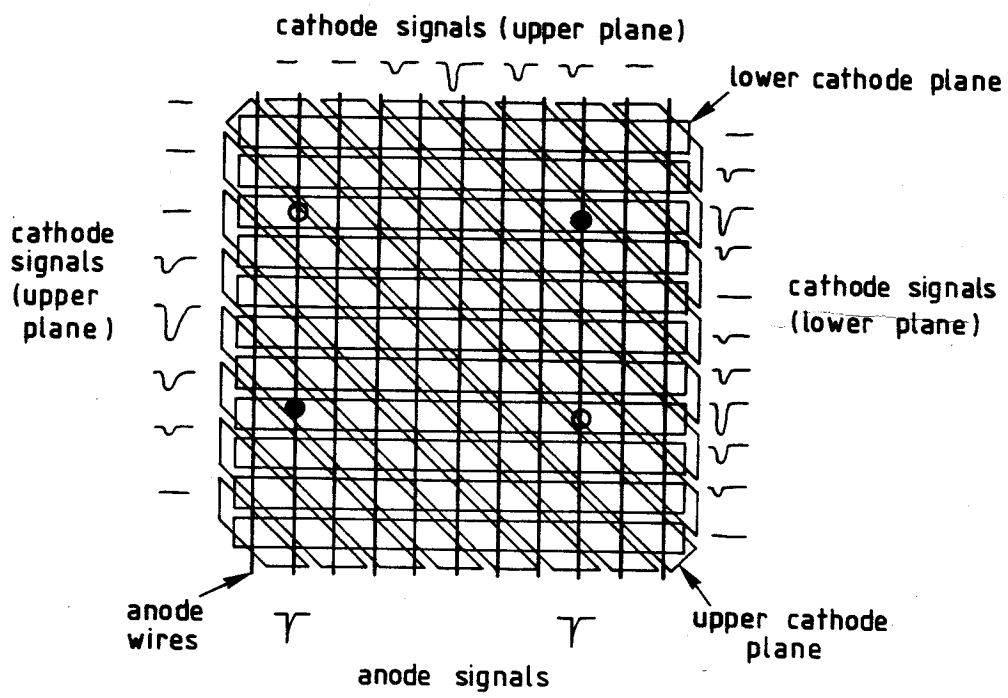
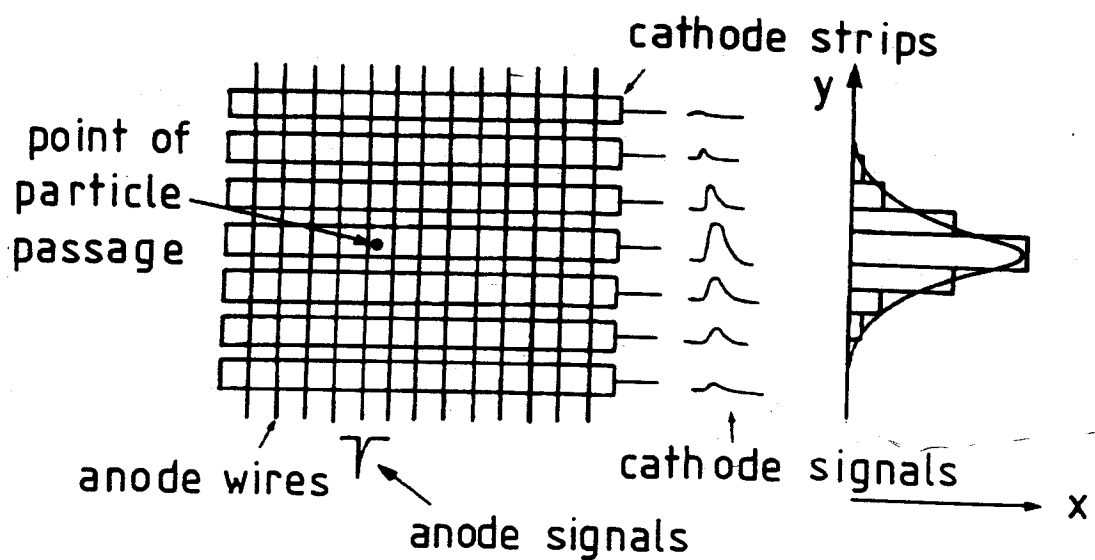


MWPC spatial resolution

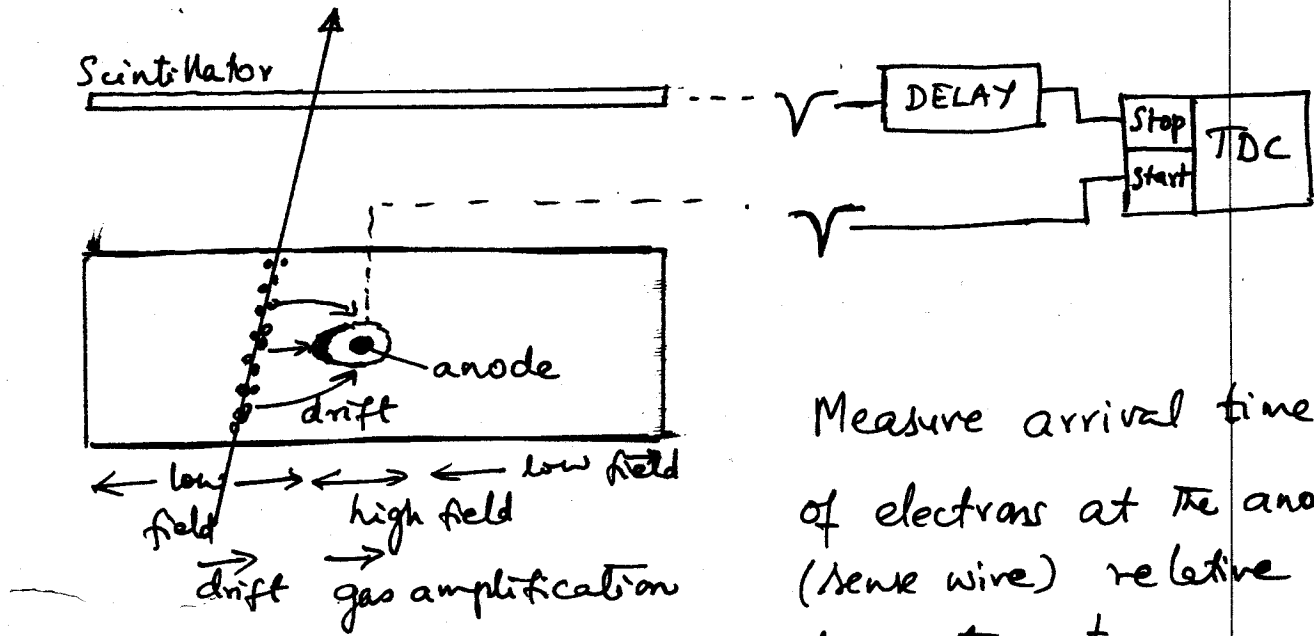
$$\sigma_z = \frac{d}{\sqrt{12}} \simeq 600 \mu\text{m} \quad (\perp^{\circ} \text{ to the anode wires})$$

no information along wire

So, improvements are made using Cathode Strips, pads or a layer of wires



DRIFT CHAMBERS



Measure arrival time
of electrons at the anode
(sense wire) relative
to a time to.

A Time "t" is required for the drift of primary electrons to reach the anode (near which gas amplification occurs).

← Depends on where the particle passed through.

Time to distance conversion

$$x = \int v_d(t) dt$$

If v_d is constant, Then $x = v_d \cdot t$.

Compared to MWPC:

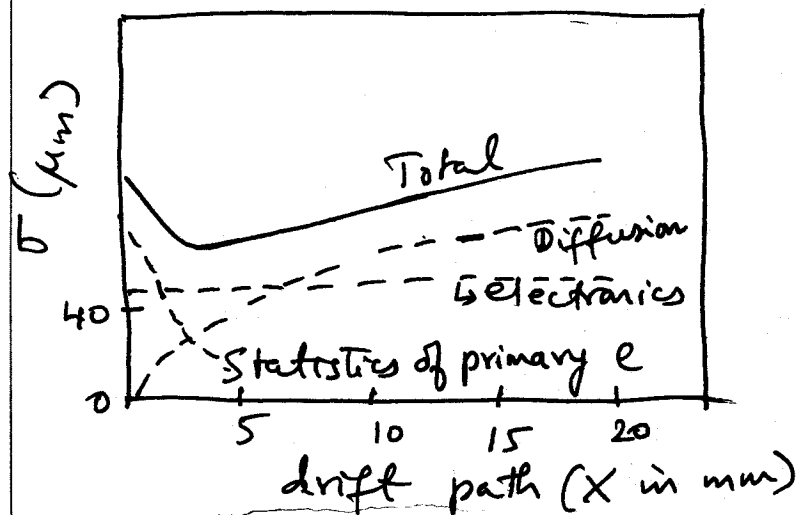
→ less number of wires, less electronics

→ better spatial resolution

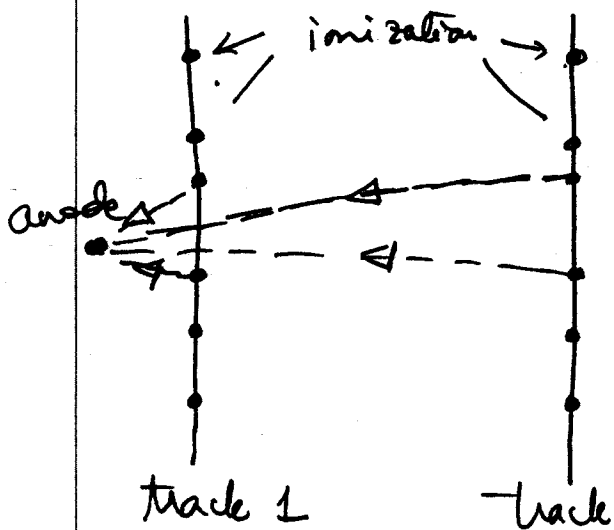
E.g., $V_0 = 5 \text{ cm}/\mu\text{s}$ (typical velocity)

with time resolution $\sim 1 \text{ ns} = \tau_t$

$$\sigma_z = v \cdot \tau_t = 50 \mu\text{m}$$



Spatial resolution has contributions from Diffusion and statistics of primary electrons (close to the anode)



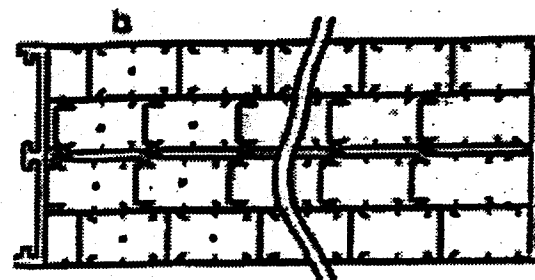
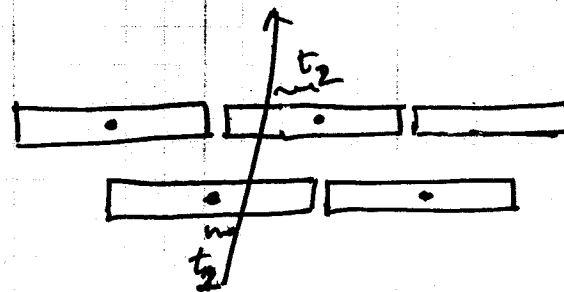
← different drift paths
for 'near' and 'distant'
particle tracks

The spatial resolution therefore depends on primary ionization statistics for near tracks.

Left-right ambiguity

The drift time measurement cannot tell us if the particle passed the anode wire on the left or the right.

So, layers are staggered.



DΦ Muon PDT

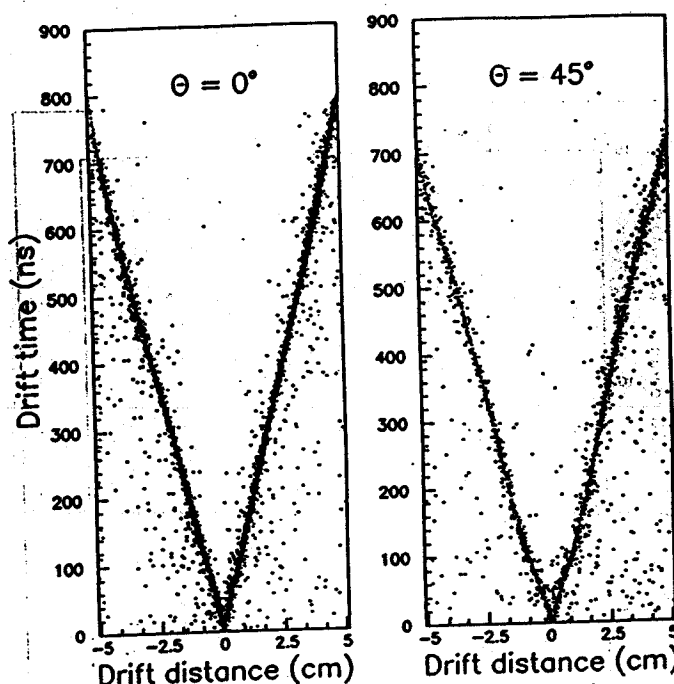
Anode:

50 μ Gold-plated tungsten
@ +4.56 kV; Cathode @ +2.3 kV

Drift-Time - to -
distance relation
almost linear.

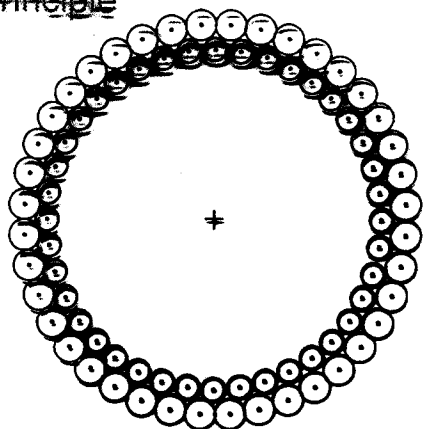
Using proper
non-linear fit

$$\Rightarrow \Gamma \sim 0.3 \text{ mm}$$



Gas used: Ar(90%) / CF₄(5%) / CO₂(5%)

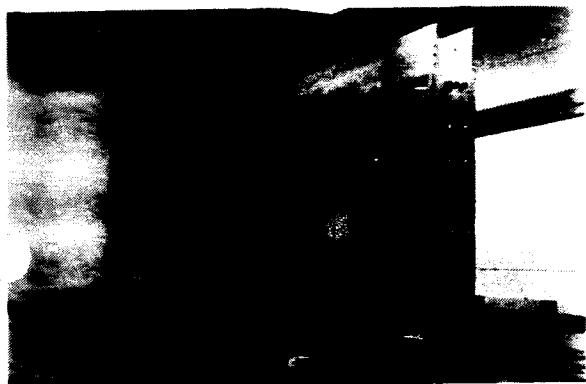
Straw tubes: Thin cylindrical cathode, 1 anode wire
principle



Example: DELPHI Inner detector

5 layers with 192 tubes each
tube \varnothing 0.9 cm, 2 m long,
wall thickness 30 μm (Al coated polyester)
wire \varnothing 40 μm
Intrinsic resolution ca. 50 μm

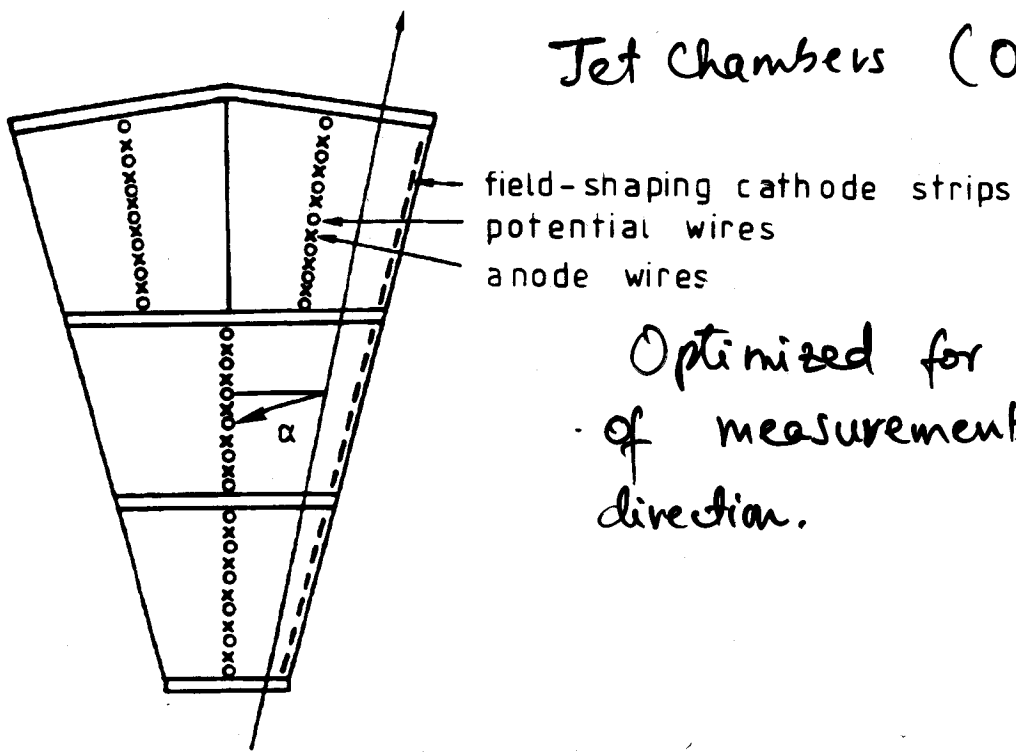
Straw tubes from C ϕ QGP Search Experiment



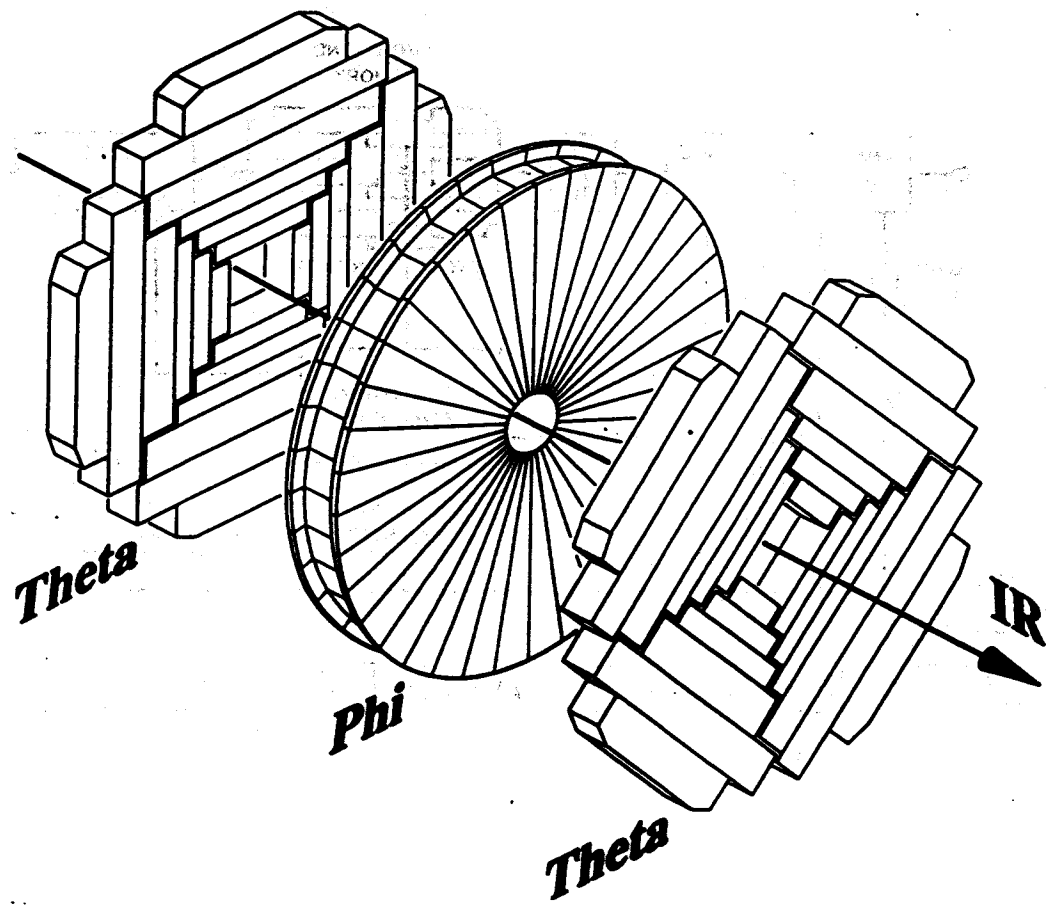
Vertical configuration for a
side or fixed-target-style
detector

particle track

Jet Chambers (OPAL for example)



Optimized for maximum number
of measurements in the radial
direction.



DΦ FDC in Run I

Figure 11

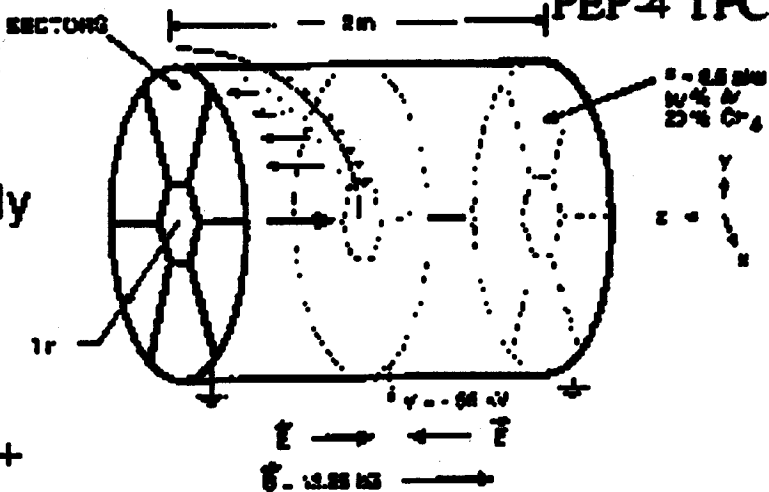
Drift Chambers

Time Projection Chamber → full 3-D track reconstruction

- ◆ x-y from wires and segmented cathode of MWPC
- ◆ z from drift time
- ◆ in addition dE/dx information

Diffusion significantly reduced by B-field.

Requires precise knowledge of $v_D \rightarrow$ LASER calibration + p,T corrections



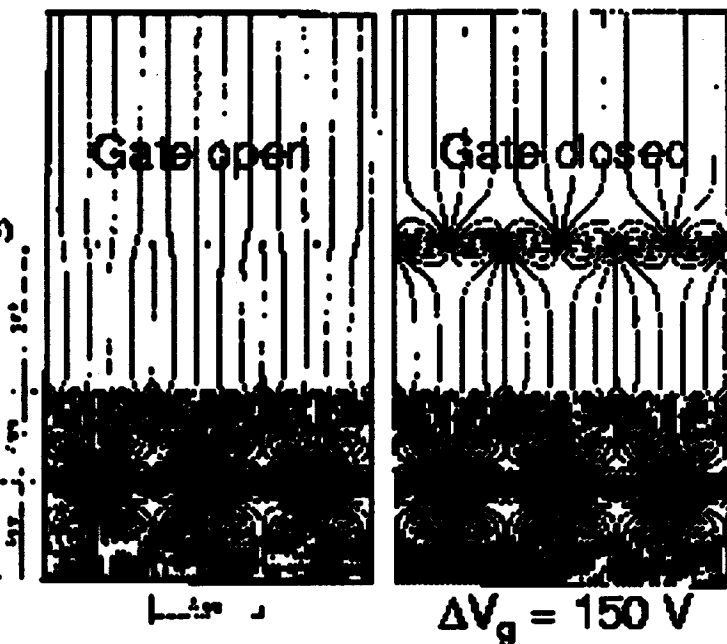
Drift over long distances → very good gas quality required

Space charge problem from positive ions, drifting back to midwall → gating

ALEPH TPC
(ALEPH coll., NIM A 294 (1990) 121,
W. Atwood et. al., NIM A 335 (1991) 445)

$\emptyset 3.6\text{M}$, $L=4.4\text{ m}$

$\sigma_{R\phi} = 173 \mu\text{m}$
 $\sigma_z = 740 \mu\text{m}$
(isolated leptons)



DETECTOR AGING

- Crucial & complex issues

Several types of effects:

- Loss of chamber gain (or increase)
- Reduction of operational region
- Loss of energy resolution
- Generation of excessive or self-sustained currents, Sparking etc
- Dark currents

Chamber aging can be defined as "deterioration in the performance of the device as a function of the irradiation time/dose."

Radiation hardness of a detector can be quantitatively calibrated using "charge accumulated /cm of anode wire"

$$\frac{Q}{\Delta l} = \frac{1}{\Delta l} \int i dt$$

Causes / Mechanisms of aging

- Decomposition of chamber gas
 - quenching gases that dissociate at the cathode get used up; change gas composition
 - molecules (such as CF_4) break-up can produce highly aggressive radicals
 - dissociation of the quencher gas at the cathode can result in polymerization and deposition of non-conducting material on the cathode
- Gas Contamination
 - Very small contaminations can have very large effects
 - Probable sources: Outgassing of various materials used in the chamber and in the gas system
- Resistive deposits on anode wires (and cathodes)

Anode deposits:

reduced and inhomogeneous field
Variation in gain (rate-dependent)

Cathode deposits:

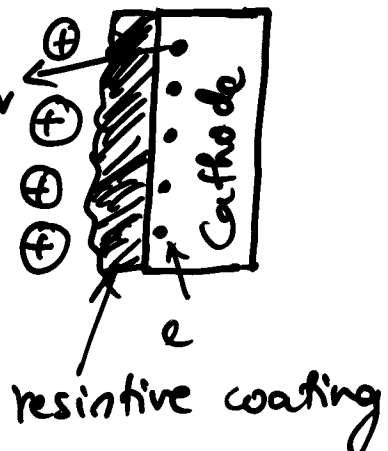
Formation of strong electric dipoles
due to ions that cannot
neutralize quickly and mirror
charge

→ Malter effect

→ field emission of electrons

→ dark current

(discharge even when the original source
is removed)



DΦ Muon PDTs

Wires got coated with crud in Run I
Chamber performances deteriorated,
some dead

Source identified as the Glassteel polyester-
epoxy resin from the cathode pad

Soln: Heating the wire in <2 ms. to near MP of gold!

Aging can be minimized by

- Careful material selection
- Cleanliness during construction and operation (clean gas systems)
- Aging-resistant gases
- Minimize impurities
- Lots of monitoring

SEMICONDUCTOR DETECTORS

- Semiconductor detectors are essentially ionization detectors with solid medium.
- Charged particles or photons produce electron-hole pairs in the semiconducting material; an electric field applied across allows the charges to be collected.

For Si, $W(e^-; \text{hole}) = 3.6 \text{ eV}$ { About 30eV
for Ge, $\rightarrow 2.8 \text{ eV}$ { in gases.

∴ Lot more primary ionization!

- Because of their high density (2.33 gm/cm^3 for Si),

$$\Delta E \text{ for MIPs} \sim 390 \text{ eV/cm} \text{ or} \\ \approx 108 \text{ e-h/cm}$$

That is 3.8 MeV/cm while for Ar $\Delta E \sim .0025 \text{ MeV/cm}$

∴ $> 10^6$ charge-carriers in Si ; $\sim 100/\text{cm}$ in Ar

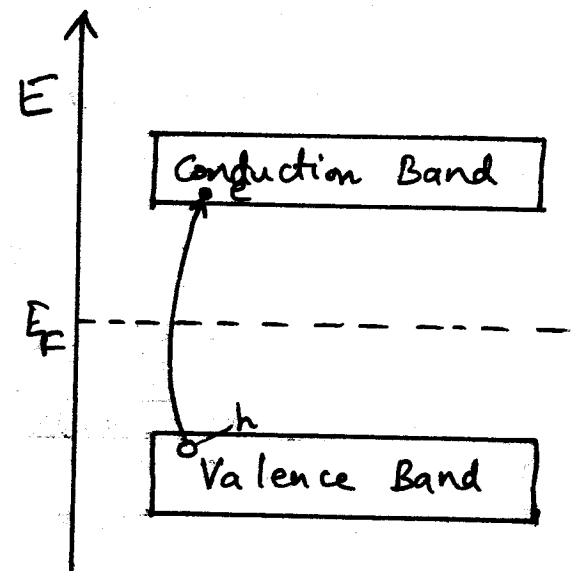
No charge multiplication mechanism (not necessary!)

Typical thickness $\sim 300 \mu\text{m} \rightarrow 3.2 \times 10^4 \text{ e-h}$

- So thin detectors possible & the rigidity allows self-supporting structures.

- High mobility
 $\mu_e = 1450 \text{ cm}^2/\text{Vs}$; $\mu_{h^+} = 450 \text{ cm}^2/\text{Vs}$
- Because of the low W -value, solid-state detectors provide excellent energy resolution.
↳ Large statistics of produced charges
- Small range of δ -electrons \Rightarrow good position measurement
- Small dimensions \rightarrow fast charge collection ($< 10\text{ ns}$)

Basic Semiconductor Physics



$$E_F = \frac{E_C + E_V}{2}$$

for intrinsic semiconductor

for single atoms in semi-conductors only discrete energy levels are available for electrons.

But, when they condense in crystalline form and a solid body, the discrete energy levels merge to form conduction and valence bands, with an energy gap between them.

Si : Band gap $\approx 1.1\text{ eV}$ } at RT

Ge : Band gap $= 0.67\text{ eV}$

(Ge detectors are cooled to reduce thermal noise)

→ Pure Silicon is an "intrinsic" semiconductor.

At $T = 0^\circ\text{K}$, the valence band is completely full
The conduction band is completely empty

No conduction. → Perfect Insulator

At elevated temperatures, thermal excitation of electrons from VB to CB.

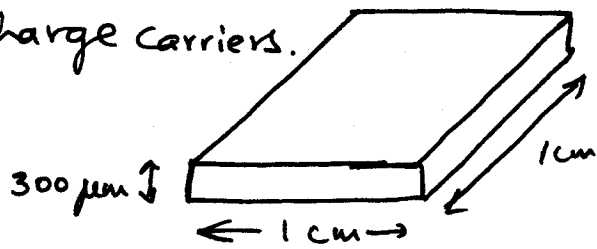
charge carrier density at RT $\approx 1.45 \times 10^{10} / \text{cc}$

of Si atoms $\approx 5 \times 10^{22} / \text{cc}$

$$n_i = 1.45 \times 10^{10} / \text{cc}$$

So, in a strip 300 μm thick

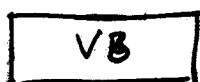
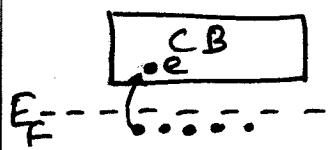
$$n_i = 4.5 \times 10^8 \text{ free charge carriers.}$$



But, only 3.2×10^4 e-h pairs
are produced by MIP.

∴ Reduce the number of free charge carriers,
i.e., deplete the detector

Doping:



n-type:

Add elements from the V group of periodic table

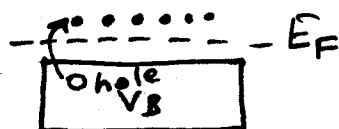
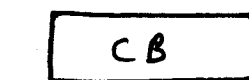
Donors \rightarrow donate electrons

that move to the CB

e^- majority carriers

E.g., Phosphorous
Arsenic

Typical doping levels:



p-type:

Add elements from III group

Acceptors: \rightarrow accept electrons creating holes.

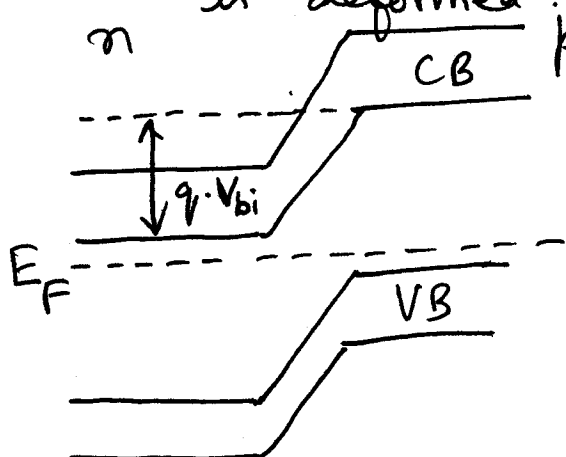
h: majority carriers

E.g.: Boron

$10^{12}/\text{cc} - 10^{15}/\text{cc}$
for detector silicon

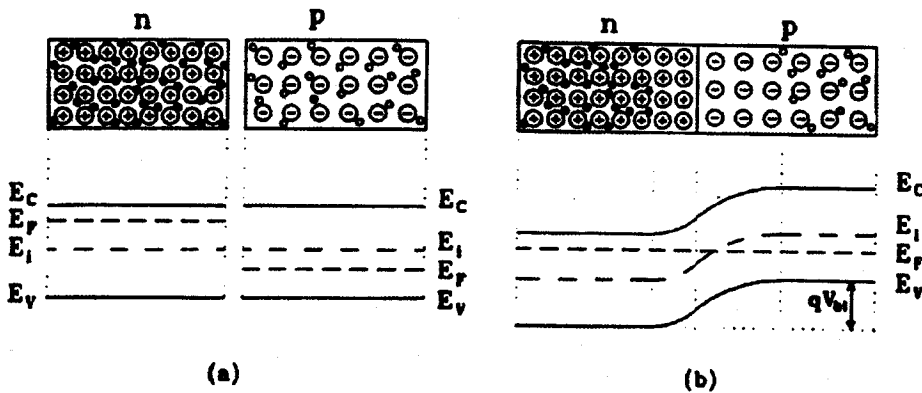
When the two types are joined, the band structure

is deformed.



Pn junction

A built-in voltage V_{bi} generated by electron and hole diffusion.



From the requirement that the Fermi levels have to match up in thermal equilibrium, the width of the space charge region becomes,

$$d = \sqrt{\frac{2\epsilon\epsilon_0}{e} \left[\frac{N_A + N_D}{N_A N_D} \right] \cdot V_{bi}}$$

$N_A, N_D \equiv$ Acceptor, donor doping concentrations

if $N_A >> N_D$ ($p^+ n$ junction)

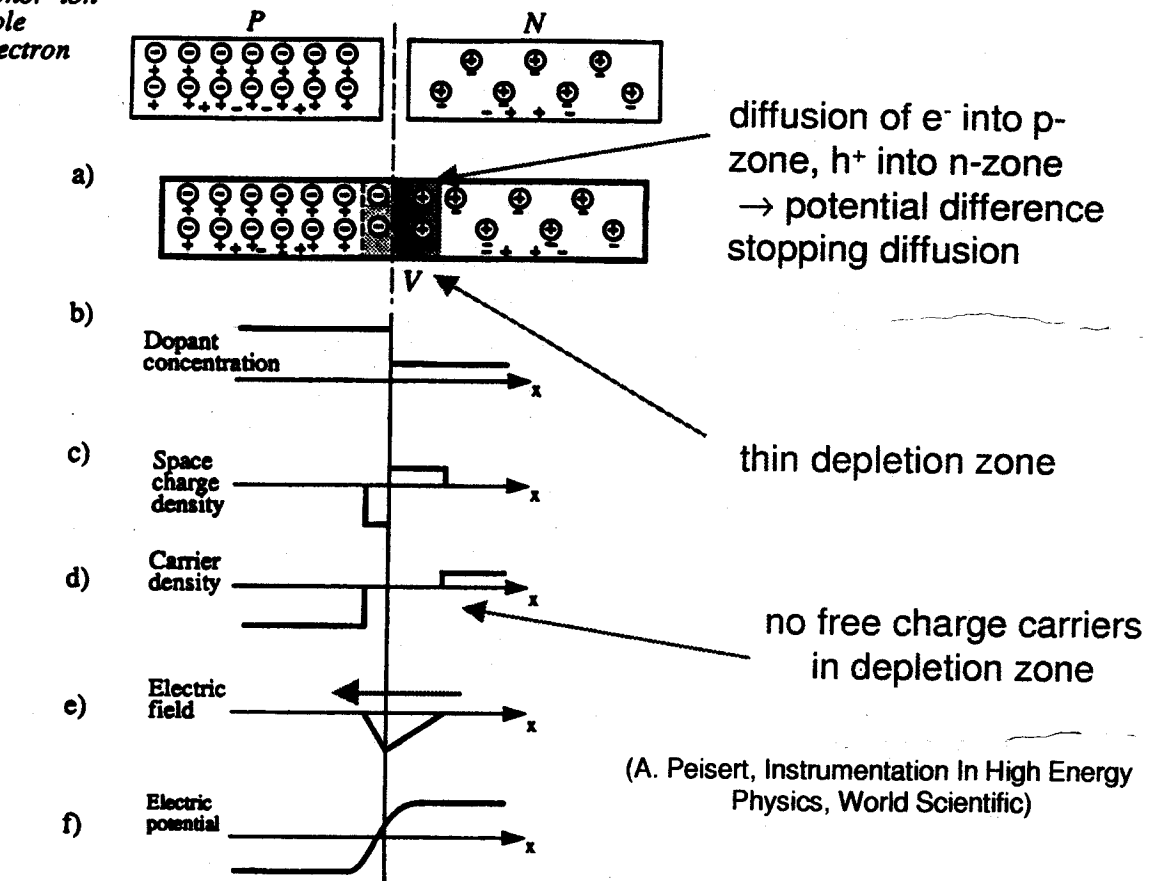
$$d \approx \sqrt{\frac{2\epsilon\epsilon_0}{e N_D} \cdot V_{bi}}$$

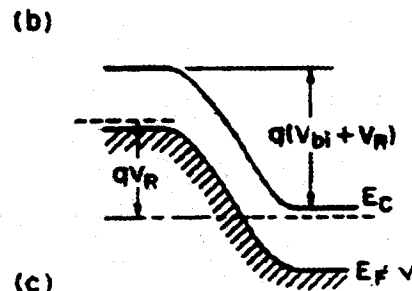
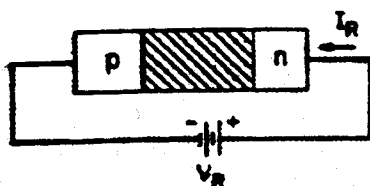
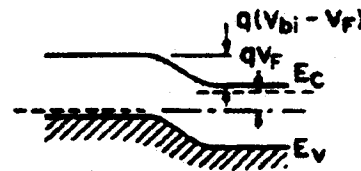
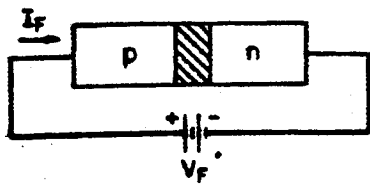
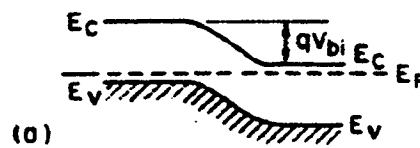
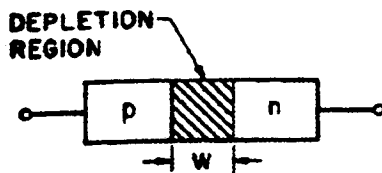
For $N_A = 10^{16}/\text{cc}$, $N_D = 10^{12}/\text{cc}$, $V_{bi} \approx 0.46V$

and $d \approx 25 \mu\text{m}$.

⊖ Acceptor ion
 ⊕ Donor ion
 + Hole
 - Electron

THE PN JUNCTION



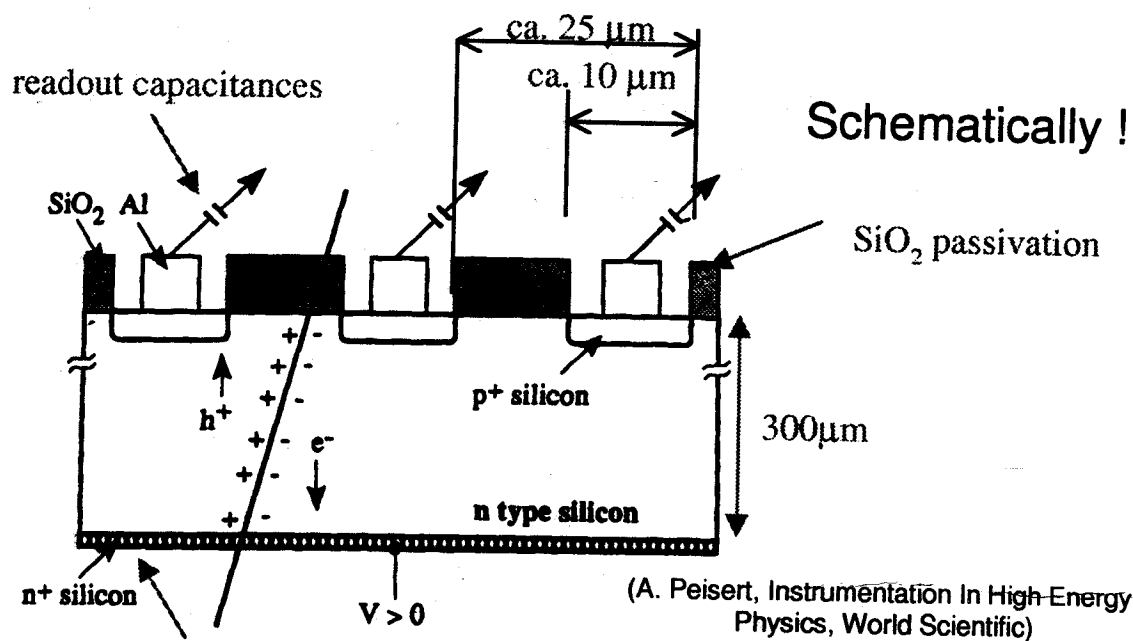


- In the reverse-bias mode, (~ 100 V) the depletion zone can extend over the full junction \rightarrow fully depleted.

$$d = \sqrt{\frac{2\epsilon\epsilon_0}{eN_D} (V_{bi} - V_R)} = \sqrt{2\epsilon\epsilon_0\mu_e p_n (V_{bi} - V_R)}$$

μ_e = mobility of e

p_n = resistivity of n-type silicon



Single-sided microstrip detector
 Spatial information obtained by segmenting
 the p-doped layer

Double-sided microstrip detectors are made
 by segmenting also the n-doped layer.

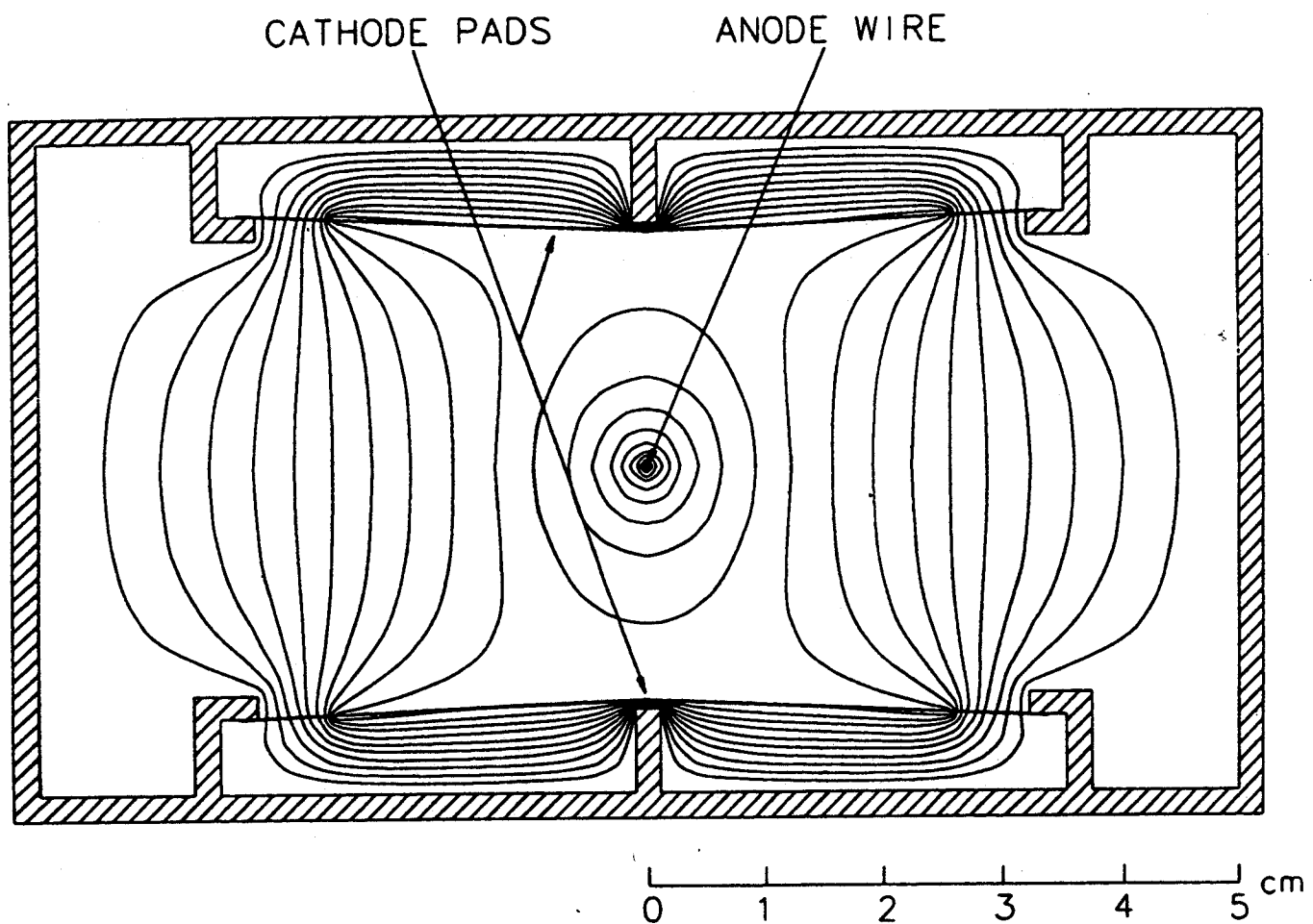
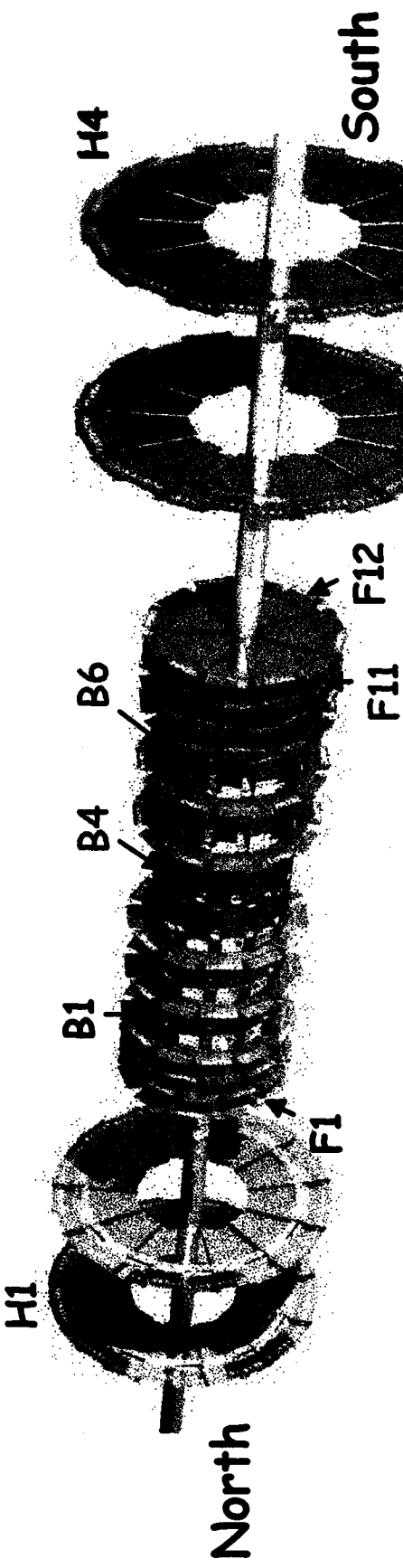


Figure 55

D \emptyset Silicon Detector

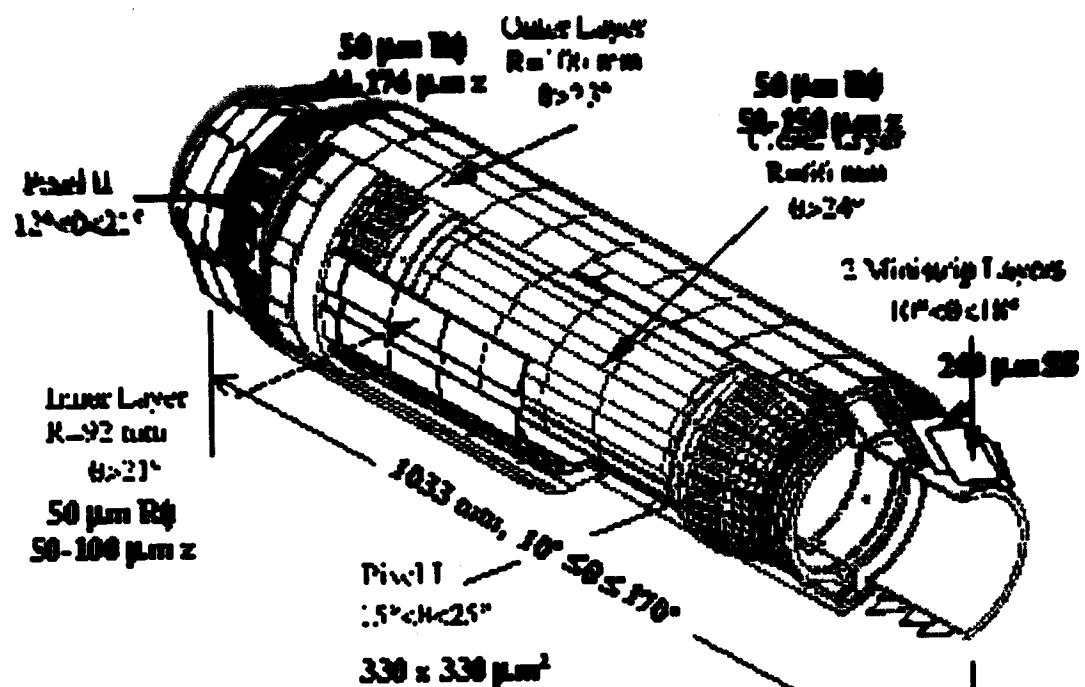


6 barrel segments in z
4 detector layers / barrel

12 small, 4 large disks

Barrels & f disks - 50 & 62.5 μm pitch
 \Rightarrow spatial resolution of 10 μm

• The DELPHI micro vertex detector (since 1992)



readout channels

ca. 174 k strips, 1.2 M pixels

total readout time: 1.6 ms

Total dissipated power

$400 \text{ W} \rightarrow$ water cooling
system

Hit resolution in

barrel part $\approx 10 \mu\text{m}$

Impact parameter
resolution (r_ϕ)

$$28 \mu\text{m} \oplus 71 \left(p \sin^2 \theta \right)$$